Characteristics of the PVC rotor R4-11 for the O4 NCal system VIR-0309A-24

Florian Aubin, Eddy Dangelser, Benoit Mours,
Antoine Syx, Pierre Van Hove

IPHC-Strasbourg

March 28, 2024

Contents

1 Introduction

This note discusses the metrology of a rotor machined at IPHC from the first batch of PVC material and follows a similar discussion made on the PVC rotor R4-10 in VIR-0203A-24 and the aluminum rotors R4-01 in VIR-0591C-22 and R4-05 in VIR-0859A-22. The drawings and figures of the PVC rotor can be found at the end of the R4-10 technical note. The rotor has been engraved IPHC-R4-11 on one side and painted on the other side.

2 Measurement method

To determine the geometry of the rotor we will use the same method as for R4-10 (see VIR-0203A-24). The thickness was measured using 16*2 = 32 points for the sectors and 8*2 = 16 points for the inner part. The outer diameter was measured using 4*3 = 12 points. The measurement points are shown in fig. 1. We will use the drawing values for the inner diameter.

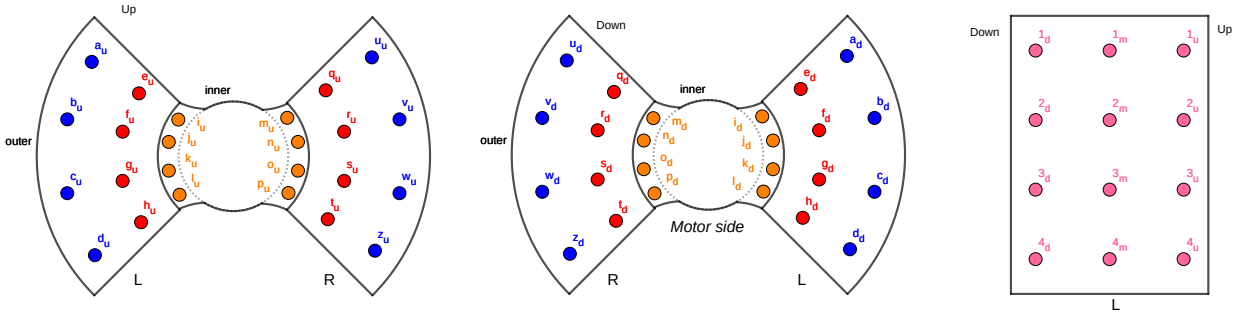

Figure 1: Outline of the faces of the rotor with the measurement points. Left is face up, center is face down and right is the side view of the left sector. Sectors have been labelled L for left sector and R for right sector.

The tool used to measure the thickness and the outer diameter is a measuring column "Garant 44 5350_600 HC1" (see VIR-0160A-22) with a given precision of 1.8+L/600 μm (L the measured length in mm). Steel reference blocks of 100.000 mm and 90.000 mm (see certificate of inspection provided at the end of this note) were used to check the accuracy of the measuring column, the standard deviation from the nominal values is of the order of the uncertainty of the measuring column (2 μm).

The measuring column was operated on a metrology table with surface defects ranging from 0 to 2 μm. The rms of the 16 values is 0.9 μm.

We measured the opening angles of the sectors using a video measuring microscope "Garant MM2" (see VIR-0591C-22) with a given precision of 2.9+L/100 μm at 95% CL (L the measured length in mm).

2.1 Thermal effects and density

The rotor R4-12 has been machined from the same PVC block (see VIR-0193A-24) as R4-10 described in VIR-0859A-22. As for R4-10 the results will be expressed at a reference temperature of 23 ± 1.5°C.

3 Raw measurements of the rotor

This section presents the raw measurements made on the rotor at the ambient temperature of 21.4°C for the thickness and 21.3°C for the diameter. Table 1 shows the thickness measurements according to the

measurement points defined in fig. 1. The rotor is laying on the table. The rotor surface as well as the table are not perfectly flat. Some space could be present in between that should be substracted when computing the rotor thickness as discussed later.

Measurement point	L sector		Measurement point	R sector	
	Up	Down		Up	Down
a	104.387	104.408	q	104.394	104.410
b	104.391	104.405	r	104.390	104.408
c	104.390	104.405	s	104.387	104.408
d	104.384	104.405	t	104.390	104.407
e	104.401	104.392	u	104.405	104.396
f	104.402	104.390	v	104.403	104.399
g	104.401	104.389	w	104.404	104.398
h	104.403	104.391	z	104.404	104.394
i	101.575	101.412	m	101.574	101.414
j	101.573	101.410	n	101.571	101.412
k	101.570	101.410	o	101.568	101.414
l	101.569	101.412	p	101.568	101.411

Table 1: Raw measurements of the height in mm for each point at 21.4°C on L and R sectors of R4-11.

Table 2 displays the diameter measurements. The measurements were made on 4*3 diameters (three parts of each diameter, the up, middle and down sides of the rotor).

Measurement point	Up	Middle	Down
1	207.353	207.352	207.342
2	207.353	207.352	207.344
3	207.353	207.350	207.344
4	207.351	207.350	207.344

Table 2: Raw measurements of the diameter in mm for each point at 21.3°C on R4-11.

Theoretical values were taken for the inner radius $r_{\text{min}} = 29$ mm and the radius for the counterweight $r_{\text{counterweight}} = 40$ mm (see drawing at the end of this note).

4 Extracting the geometrical parameters

4.1 Thickness

We need to correct the possible gap between the rotor and the measuring table. Assuming that the table is flatter than the rotor surface we can extract the gap from the measurement of the top surface considering the plane tangents to the highest points (asking them to be on both sectors). For this rotor these points are e, q, t for the up and e, q, s for the down face (see fig. 1). Using the measurements in table 1 we can compute a plane equation for each side of the rotor in cartesian coordinates:

$$\text{Up plane equation} : z = 2.07 \times 10^{-5}x - 4.83 \times 10^{-5}y + 104.407 \quad (1)$$

$$\text{Down plane equation} : z = 5.37 \times 10^{-5}x - 5.88 \times 10^{-5}y + 104.406 \quad (2)$$

Using eqs. (1) and (2) the gap can be determined, see table 3. The maximum rms of the gap for a sector is 7.9 μm.

Measurement point	L sector		Measurement point	R sector	
	Up	Down		Up	Down
a	21	11	q	2	0
b	15	12	r	4	1
c	15	13	s	3	0
d	19	9	t	2	-1
e	7	0	u	19	17
f	5	0	v	20	12
g	5	-2	w	19	11
h	2	-3	z	15	13

Table 3: Gap computed in μm on up and down sides of both sectors of R4-11.

We can then compute the rotor thickness for each point by removing these gaps. If one of the raw values is lower than the corrected thickness we take this lowest value. The thickness of the inner part is computed by taking into account the air between the closest measurement point on the sector and the measurement point on this part, the average value between up and down is taken as our final value. The value of each point is shown in table 4 at 23°C.

Measurement point	L sector	Measurement point	R sector
a	104.400	q	104.421
b	104.403	r	104.418
c	104.400	s	104.418
d	104.397	t	104.418
e	104.414	u	104.405
f	104.415	v	104.403
g	104.413	w	104.402
h	104.414	z	104.404
i	98.597	m	98.592
j	98.593	n	98.593
k	98.590	o	98.584
l	98.590	p	98.581

Table 4: Measurements of the thickness in mm for each point at 23°C on L and R sectors of R4-11.

4.2 Radius

Using comparators while the rotor is rotating on its axis we can determine the deformation on both sectors and compute different radii values. Table 5 shows the raw measurements using comparators on L and R sectors. The measurements were made on the up, middle and down sides of L and R sectors using three comparators for a total of 5*3*2=30 points (the first and last points are near the edge of the sectors).

Measurement point	L sector			R sector		
	Up	Middle	Down	Up	Middle	Down
A	-12	-24	-30	0	-2	0
B	-10	-18	-24	-5	-10	-10
C	-5	-10	-17	-10	-18	-20
D	0	-4	-10	-15	-24	-28
E	0	0	0	-20	-28	-35

Table 5: Raw measurements in μm of the comparators for the L and R sectors of R4-11.

The zeroing of the comparators was made arbitrarily close to the edge of the sector. The offsets shown in table 5 are measured relative to this reference.

To compute the radius per measurement point we use the following process: First we compute the mean deformation for one comparator. Then we remove this mean deformation to each measurement of this comparator. The corrected shift value is added to the mean of the associated up, middle or down diameter computed using table 2 at 21.3°C. This process is repeated for each comparator. The final radius for each point are shown in table 6.

Measurement point	L sector			R sector		
	Up	Center	Down	Up	Center	Down
A	103.672	103.665	103.659	103.684	103.687	103.689
B	103.674	103.671	103.665	103.679	103.679	103.679
C	103.679	103.679	103.672	103.674	103.671	103.669
D	103.679	103.685	103.679	103.669	103.665	103.661
E	103.684	103.689	103.689	103.664	103.661	103.654

Table 6: Radius measurements in mm at 21.3°C for the L and R sectors of R4-11.

5 Characterization of the rotor using a simple model

5.1 Theoretical model of the rotor

Using the analytical strain equation at 2f shown in eq. (3) with the rotor design parameters at a distance of 1.7 m, an angle to beam axis of $34.7°$ and a twist angle of $12°$ we compute a value of $1.1480 \times 10^{-18}/(2f_{rot})^2$.

$$h_{2f}(\psi) = \frac{G\rho_{rot}\ b\ sin(\alpha)(r_{max}^4 - r_{min}^4)}{32L\pi^2 f_{2rot}^2}\ (9\cos^2\psi\cos\phi + 6\cos\psi\sin\psi\sin\phi) \tag{3}$$

When using FROMAGE v1r2 with the same parameters we obtain $1.1415 \times 10^{-18}/(2f_{rot})^2$. The 0.569% between both results is due to the mirror and rotor finite element geometry computed in FROMAGE.

At 2.1 m the difference between the analytical formula and FROMAGE is 0.373% as it converges to the point mass approximation when the distance increases.

5.2 Thickness

A simple model can be used to determine a mean value for the thickness and its uncertainty.

As shown on fig. 1, a total of $16 + 8 = 24$ points were used to compute the thickness of each sector.

For the simple model we take the thickness as the mean value of table 4: 104.409 mm at 23°C. Since we have a limited number of measurement points, to be conservative we take the thickness uncertainty as the rms of table 4 (7.9 μm) to which we add linearly the metrology table uncertainty (0.9 μm) and the tool uncertainty (2.0 μm). Therefore, for this simple model, the thickness is 104.409 $\pm$ 0.011 mm.

5.3 Radius

For the simple model we take the radius as the mean value of table 6: 103.688 mm at 23°C. Using a linear sum of the rms of table 6 (9.7 μm) and the tool uncertainty (2.2 μm) we take an uncertainty of 12 μm on the mean radius.

5.4 Expected NCal signal and uncertainties

The simple model geometry used to describe this rotor is represented in fig. 2. As for R4-10 (see section 5.4 of VIR-0859A-22) we take into account the housing space for the counterweights on each side of the rotor as seen in the drawing at the end of the R4-10 technical note, each space is 3 mm thick and 40 mm of radius wide.

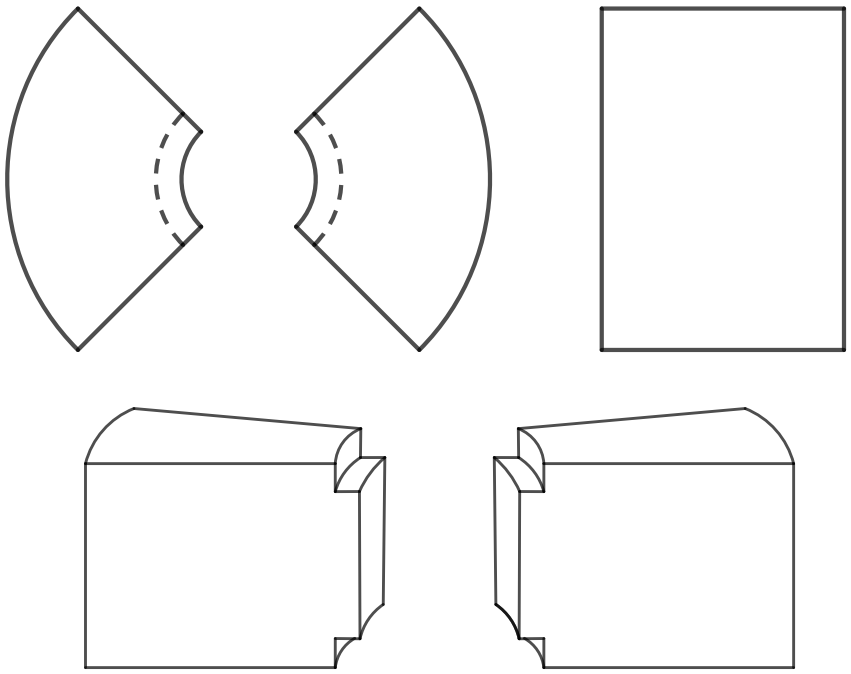

Figure 2: Simple model geometry including the counterweight spacings. Left top is a top view, right top is a side view (external sector) and bottom is a tilted view of the rotor.

Using FROMAGE on this geometry we compute the following 2f strain on the mirror at a distance of 1.7 m, an angle to beam axis of 34.7° and a twist angle of 12°:

- strain(2f) = $\dfrac{1.1269 \times 10^{-18}}{(2f_{rot})^2}$

This last value will be compared to the advanced model.

The uncertainties considered for this model are displayed in table 7.

R4-11 rotor parameter simple model (23°C)			NCal 2f signal uncertainty	
name	value	uncertainty	formula	value (%)
Density ρ (kg.m^{-3})	1442.3	0.2	$\delta\rho/\rho$	0.014
Thickness b (mm)	104.409	1.1×10^{-2}	$\delta b/b$	0.010
r_{max} (mm)	103.688	1.2×10^{-2}	$4\delta r_{max}/r_{max}$	0.046
G (m^3.kg^{-1}.s^{-2})	$6.674\,30 \times 10^{-11}$	1.5×10^{-15}	$\delta G/G$	0.002
Temperature T (°C)	23	1.5	$\left\|\frac{\partial h}{\partial T}\right\| \frac{\Delta T}{h}$	0.024
Quadratic sum				0.054

Table 7: Uncertainties on the amplitude of the calibration signal at 2f from the R4-11 rotor simple model geometry.

6 Characterization of the rotor using an advanced model

6.1 Thickness

A more advanced model can be used considering the deformations on the surfaces of the sectors for better accuracy. Each measurement point of table 4 can be considered as a sub-sector with its own thickness.

The uncertainty on this value is more complex to evaluate. As a conservative approach we use the maximum rms of the deviation to a plane for each sector (7.9 µm see section 4.1) to which we add linearly the uncertainty on the flatness of the measurement table (0.9 µm) as well as the measurement tool (2.0 µm). The total uncertainty on the thickness is 12 µm.

6.2 Radius

On fig. 1 we divided the external sectors in 4 sub-sectors for each sector (blue points). We convert the point of table 6 to the grid of fig. 1 by averaging the two closest values and converting them to 23°C. The results are shown in table 8. We notice that the L sector is on average 4 µm larger than the R sector.

Radius	L sector			R sector		
	Up	Center	Down	Up	Center	Down
1	103.697	103.682	103.676	103.696	103.697	103.698
2	103.691	103.689	103.682	103.691	103.689	103.688
3	103.693	103.696	103.689	103.686	103.682	103.679
4	103.696	103.701	103.698	103.681	103.677	103.671

Table 8: Radius measurements (in mm at 23°C) for the L and R sectors of R4-11.

The rms of the radii is 8.0 µm. The tool uncertainty is 2.2 µm. Like for the thickness we use a linear sum and find the uncertainty on both radii to be 10.2 µm.

6.3 Counterweights

A pair of counterweights have been designed to reduce the unbalance of the rotor using the same method as R4-10 in section 6.3 of VIR-0203A-24. These counterweights are made of Aluminum 2017 ($\rho_{\mathrm{Al}_{2017}} = 2790$ kg.m^{-3}). Using PVC for the counterweights would have required excessive material removal and exceeded the inner radius limit on the counterweight placed on the motor side.

Figure 3 shows the geometry of the machined counterweights to balance the rotor with a material cut following a chord of 57.09 mm (see black areas on fig. 3). the disk on the left was designed so the motor would fit in its center, the disk on the right fits the axle of the rotor. The thickness of the disks is 3 mm, with an outer radius measuring 40 mm. On the motor side, the inner radius of the disk is 21.75 mm, while on the axle side, it measures 10 mm.

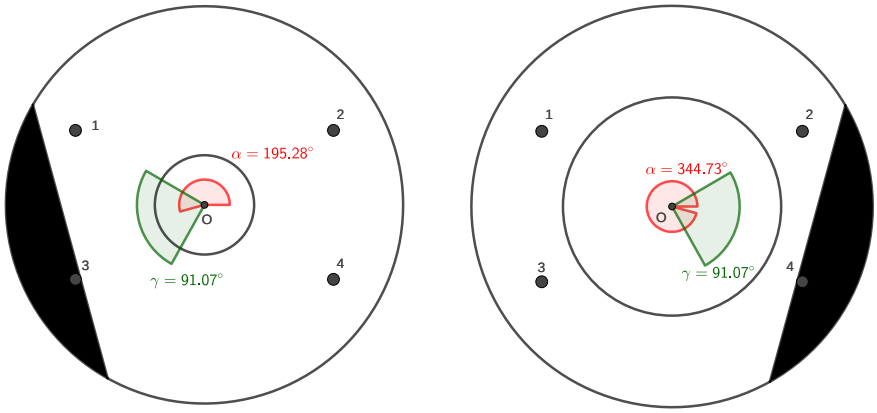

Figure 3: Outline of the counterweights for R4-12. The black areas represents the material removed.

6.4 Opening angles and asymmetry

The opening angles of the full and empty sectors have been measured using a video microscope with the same method as for R4-01.

The measurements are shown in table 9. The center value corresponds to the mean of up and down measurements.

Opening angle	Up	Center	Down
L	1.57116	1.57149	1.57181
R	1.57105	1.57111	1.57117
L-R	1.57070	1.57145	1.57220
R-L	1.57027	1.56914	1.56800

Table 9: Opening angle measurements in rad for the L, R full sectors and L-R, R-L empty sectors of R4-11.

These measurements allow us to compute the signal with different opening angles and an asymmetry between the sectors. These measured opening angles will be included in the advanced model described in the next section.

Using FROMAGE on the advanced rotor geometry we can compare the effects of the opening angles between perfectly symmetrical sectors and the values of table 9. This gives a relative difference below 0.001% on the rotor signal at 2f.

The uncertainty on α = 0.2 mrad is the same as for R4-01, we use FROMAGE to propagate it on the measurements shown in table 9 and find a relative deviation below 0.001% on the rotor signal at 2f. This value will be taken as the opening angle and asymmetry uncertainty.

6.5 Expected NCal signals and uncertainties

6.5.1 Advanced geometry including chamfers and counterweight

The geometry used to describe the rotor as an advanced model is represented in fig. 4. The external parts of the sectors are divided in 3 sub-sectors each to correspond to the different radii determined. In addition we include the counterweight, the opening angles and asymmetry of the sectors. The screws and screw holes are not taken into account since they are placed symmetrical they should not impact the 2f signal.

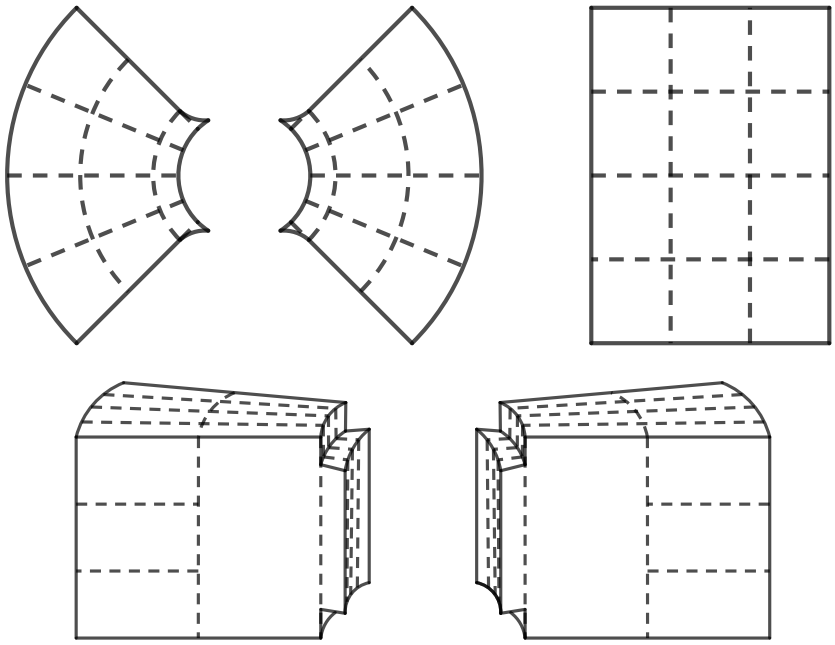

Figure 4: Advanced model geometry used to describe the rotor. Top left is a front view, top right is a side view (external sub-sectors) and bottom is a tilted view of the sectors. Only the 4 external part sectors are divided in 3 sub-sectors each. The chamfers are visible on the inner radius.

Using FROMAGE at a distance of 1.7 m, an angle of $34.7°$ and a twist of $12°$ on this geometry gives the following strains:

- strain(1f) $= \dfrac{2.3663 \times 10^{-20}}{(1 f_{rot})^2}$
- strain(2f) $= \dfrac{1.1262 \times 10^{-18}}{(2 f_{rot})^2}$

The relative deviation to the simple model at 2f is 0.062%.

6.5.2 Remaining geometry uncertainty

Other geometrical defects are probed by the remaining 1f signal computed with the advanced geometry as described for the rotor R4-01 (see section 7.5.4 of VIR-0591C-22). For this rotor the 1f signal is 3 times smaller than for R4-01. Nevertheless we will use the $5 \times 10^{-4}\%$ R4-01 remaining geometry uncertainty as a conservative approach.

6.5.3 Uncertainties

To set an uncertainty on the strain(2f) from the description of the geometry we take the difference between the simple model (strain(2f) = $1.1269 \times 10^{-18}/(2f)^2$) and the advanced model (strain(2f) = $1.1262 \times 10^{-18}/(2f)^2$). This deviation of 0.062% is reported in table 10 as modelling uncertainty.

The uncertainties considered for this full model are displayed in table 10. We point out that the elongation of the material caused by the rotation is not taken into account in this technical note.

R4-11 rotor parameter advanced model (23°C)			NCal 2f signal uncertainty	
name	mean value	uncertainty	formula	value (%)
Density ρ (kg.m^{-3})	1442.3	0.2	$\delta\rho/\rho$	0.014
Thickness b left sector (12 sub-sectors) (mm) Thickness b right sector (12 sub-sectors) (mm)	104.407 104.411	1.2×10^{-2}	$\delta b/b$	0.011
r_{max} left sector (12 ext sub-sectors) (mm) r_{max} right sector (12 ext sub-sectors) (mm)	103.690 103.686	1.0×10^{-2}	$4\delta r_{max}/r_{max}$	0.039
G (m^3.kg^{-1}.s^{-2})	$6.674\,30 \times 10^{-11}$	1.5×10^{-15}	$\delta G/G$	0.002
Temperature T (°C)	23	1.5	$\left\lvert\frac{\partial h}{\partial T}\right\rvert \frac{\Delta T}{h}$	0.024
Modelling Uncertainty				0.062
FROMAGE grid uncertainty				0.005
Opening angle and sector asymmetry uncertainty				0.001
Remaining geometry uncertainty				$<5 \times 10^{-4}$
Total uncertainty from the rotor (quadratic sum)				0.079

Table 10: Uncertainties on the amplitude of the calibration signal at 2f from the R4-11 rotor advanced model geometry at 23°C.

A Appendix

```
### This is a cfg file for a more realistic geometry of the mirror and the Virgo NCal R4-11 (2024)

### ALL THE OBJECTS ARE DEFINED IN THE MIRROR'S FRAME (O,x,y,z),
### with O the center of the mirror, x axis along the ITF's beam toward the beam-splitter,
### y axis orthogonal to x in the plane of the ITF,
### z axis orthogonal to the plane of the ITF upward

### MIRROR DEFINITION

GRID_SIZE 12 30 8

CYLINDER 2202. 0 0.175 0.2 360 0 0 0

GRID_SIZE 1 1 1

# Defining the flats on the edge of the mirror
CUT_CYL 2202. 0.175 0.2 0.05 0 0
CUT_CYL 2202. 0.175 0.2 0.05 0 180

# Defining the ears and anchors of the mirror
CUBOID 2202. 0.090 0.010 0.015  0     0.1782 -0.0125
CUBOID 2202. 0.090 0.010 0.015  0    -0.1782 -0.0125
CUBOID 2202. 0.039 0.008 0.008 -0.02 -0.1772 -0.024
CUBOID 2202. 0.039 0.008 0.008 -0.02  0.1772 -0.024
CUBOID 2202. 0.039 0.008 0.008  0.02 -0.1772 -0.024
CUBOID 2202. 0.039 0.008 0.008  0.02  0.1772 -0.024

### ROTOR DEFINITION: CYLINDER DENSITY INNER_RADIUS OUTER_RADIUS THICKNESS OPEN_ANGLE r z theta

ROTOR_CYLINDRICAL 1.7 34.7 0 0 12

### COUNTERWEIGHT AXLE
GRID_SIZE 8 17 14
CYLINDER 1442.3 0.010 0.040 0.003 360 0 0.050798309376 0
GRID_SIZE 1 1 1
CUT_CYL 1442.3 0.040 0.003 0.05709 0.050798309376 195.28

### COUNTERWEIGHT MOTOR
GRID_SIZE 8 17 14
CYLINDER 1442.3 0.02175 0.040 0.003 360 0 -0.050798309376 0
GRID_SIZE 1 1 1
CUT_CYL 1442.3 0.040 0.003 0.05709 -0.050798309376 195.28

# TRES RAPIDE
#GRID_SIZE 4 4 4
# RAPIDE
GRID_SIZE 8 17 14
# LENT
#GRID_SIZE 8 65 40

### L sector

## Inner part
OUTER_FILLET 1442.3 0.029 0.098597 0 0.01 -11.2549 146.2352
```

```
CYLINDER 1442.3 0.029 0.04 0.098597 22.5099 0 0 146.2352
CYLINDER 1442.3 0.029 0.04 0.098593 22.5099 0 0 168.7451
CYLINDER 1442.3 0.029 0.04 0.098590 22.5099 0 0 191.2549
CYLINDER 1442.3 0.029 0.04 0.098590 22.5099 0 0 213.7648
OUTER_FILLET 1442.3 0.029 0.098590 0 0.01 11.2549 213.7648

## Middle part
CYLINDER 1442.3 0.04 0.072 0.104414 22.5099 0 0 146.2352
CYLINDER 1442.3 0.04 0.072 0.104415 22.5099 0 0 168.7451
CYLINDER 1442.3 0.04 0.072 0.104413 22.5099 0 0 191.2549
CYLINDER 1442.3 0.04 0.072 0.104414 22.5099 0 0 213.7648

## Outer part
CYLINDER 1442.3 0.072 0.103687 0.034800120512 22.5052 0 0.034800120512 146.2422
CYLINDER 1442.3 0.072 0.103682 0.034800120512 22.5099 0 0 146.2352
CYLINDER 1442.3 0.072 0.103676 0.034800120512 22.5146 0 -0.034800120512 146.2281

CYLINDER 1442.3 0.072 0.103691 0.03480112064 22.5052 0 0.03480112064 168.7474
CYLINDER 1442.3 0.072 0.103689 0.03480112064 22.5099 0 0 168.7451
CYLINDER 1442.3 0.072 0.103682 0.03480112064 22.5146 0 -0.03480112064 168.7427

CYLINDER 1442.3 0.072 0.103693 0.034800120512 22.5052 0 0.034800120512 191.2526
CYLINDER 1442.3 0.072 0.103696 0.034800120512 22.5099 0 0 191.2549
CYLINDER 1442.3 0.072 0.103689 0.034800120512 22.5146 0 -0.034800120512 191.2573

CYLINDER 1442.3 0.072 0.103696 0.034799120384 22.5052 0 0.034799120384 213.7578
CYLINDER 1442.3 0.072 0.103701 0.034799120384 22.5099 0 0 213.7648
CYLINDER 1442.3 0.072 0.103698 0.034799120384 22.5146 0 -0.034799120384 213.7719

### R sector

## Inner part
OUTER_FILLET 1442.3 0.029 0.098592 0 0.01 11.2522 33.6908
CYLINDER 1442.3 0.029 0.04 0.098592 22.5044 0 0 33.6908
CYLINDER 1442.3 0.029 0.04 0.098589 22.5044 0 0 11.1863
CYLINDER 1442.3 0.029 0.04 0.098588 22.5044 0 0 348.6819
CYLINDER 1442.3 0.029 0.04 0.098586 22.5044 0 0 326.1774
OUTER_FILLET 1442.3 0.029 0.098586 0 0.01 -11.2522 326.1774

## Middle part
CYLINDER 1442.3 0.04 0.072 0.104421 22.5044 0 0 33.6908
CYLINDER 1442.3 0.04 0.072 0.104418 22.5044 0 0 11.1863
CYLINDER 1442.3 0.04 0.072 0.104418 22.5044 0 0 348.6819
CYLINDER 1442.3 0.04 0.072 0.104418 22.5044 0 0 326.1774

## Outer part
CYLINDER 1442.3 0.072 0.103696 0.034801787392 22.5036 0 0.034801787392 33.6895
CYLINDER 1442.3 0.072 0.103697 0.034801787392 22.5044 0 0 33.6908
CYLINDER 1442.3 0.072 0.103698 0.034801787392 22.5053 0 -0.034801787392 33.6920

CYLINDER 1442.3 0.072 0.103691 0.03480112064 22.5036 0 0.03480112064 11.1859
CYLINDER 1442.3 0.072 0.103689 0.03480112064 22.5044 0 0 11.1863
CYLINDER 1442.3 0.072 0.103688 0.03480112064 22.5053 0 -0.03480112064 11.1867

CYLINDER 1442.3 0.072 0.103686 0.034800787264 22.5036 0 0.034800787264 348.6823
CYLINDER 1442.3 0.072 0.103682 0.034800787264 22.5044 0 0 348.6819
```

```
CYLINDER 1442.3 0.072 0.103679 0.034800787264 22.5053 0 -0.034800787264 348.6815

CYLINDER 1442.3 0.072 0.103681 0.034801454016 22.5036 0 0.034801454016 326.1787
CYLINDER 1442.3 0.072 0.103677 0.034801454016 22.5044 0 0 326.1774
CYLINDER 1442.3 0.072 0.103671 0.034801454016 22.5053 0 -0.034801454016 326.1762

### GENERAL PARAMETERS

STEP 22.5 16

ARM_LENGTH 3000

SIGNAL 2
```